JOURNAL OF CATALYSIS 77, 1–15 (1982)

Hydrogenation of CO to Methane: Kinetic Studies on Polycrystalline Nickel Foils

R. S. POLIZZOTTI AND J. A. SCHWARZ[1]

Department of Corporate Research, Exxon Research & Engineering Company, P.O. Box 45, Linden, New Jersey 07036

Received January 26, 1981; revised December 30, 1981

The existence of a transition in the activation energy of the methanation reaction, a decrease in the activation energy with increasing H_2/CO ratio below the transition, a shift of the transition to lower temperature with increasing H_2/CO ratio, and the existence of a kinetic isotope effect for the reaction at low pressure and high H_2/CO ratio have been shown. This kinetic behavior can be understood in terms of the temperature and partial-pressure dependence of the hydrogen adatom surface concentration. The observation of a kinetic isotope effect and the correlation between the kinetic behavior of the calculated hydrogen adatom surface concentration and the observed kinetics of the methanation reaction suggest that the methanation reaction over nickel is a hydrogen adatom surface concentration-limited reaction.

INTRODUCTION

Sixty-six years ago nickel was discovered to be an effective catalyst for the synthesis of methane from carbon monoxide and hydrogen. Despite the numerous studies carried out since that discovery, the mechanism of the synthesis is still controversial. Recent reviews (*1–3*) have summarized the results of these studies. With the advent of tools combining ultrahigh vacuum (UHV) surface characterization with atmospheric-pressure chemical reactors, it has become possible to study the kinetics of heterogeneously catalyzed reactions over a broad range of reaction conditions on well-characterized metal surfaces free from support effects and possible diffusional limitations. Metallic catalysts in the form of polycrystalline foils and single crystals whose chemisorption properties have been studied by a wide variety of (UHV) techniques can now be used routinely in kinetic studies of heterogeneously catalyzed reactions. Surface characterization before and after reaction combined with kinetic studies of the reaction over a wide range of reaction conditions can be performed. Studies of the coadsorption of reactants and products on well-characterized low-surface-area metallic catalysts are providing new insights into the reaction mechanisms for methane synthesis over Group VIII metals. In the present studies, the kinetics of the hydrogenation of CO to methane over polycrystalline nickel foils are measured for H_2/CO ratios from 1/1 to 30/1, total reactant pressures between 5 and 200 Torr, and reaction temperatures between 150 and 400°C. One objective of this work was to define the kinetic behavior of the methanation reaction, over a well-characterized nickel surface, for a broad range of reaction conditions in order to provide a basis for comparison of the various proposed kinetic models. The data show that a reversible transition in the temperature dependence of the methanation reaction rate exists. The transition is characterized by a change in both the activation energy and the partial-pressure dependence of the reaction. The transition between the two kinetic regimes

[1] Current address: Department of Chemical Engineering and Materials Science, Syracuse University, Syracuse, N.Y. 13210. To whom all correspondence should be addressed.

0021-9517/82/090001-15$02.00/0

shifts to lower temperature as the H_2/CO ratio increases at fixed total reactant pressure. In addition, it is found that the activation energy of the reaction below the transition is not constant but decreases as the H_2/CO ratio increases.

Little agreement exists in the literature over whether a kinetic isotope effect exists for the methanation reaction over the Group VIII metals (*4–6*). Measurement of the kinetic isotope effect by Dalla Betta and Shelef (*4*) on supported nickel catalysts show no measurable change in the methanation rate on replacement of H_2 by D_2. The lack of an observed isotope effect has strongly supported the view that CO dissociation is rate determining in the methanation reaction on the nickel surface. Ozaki (*7*) and Wilson (*8*) have pointed out that the failure to observe an isotope effect could be due to cancellation of the kinetic and thermodynamic effects for the range of reaction conditions used. Measurements of the H_2/D_2 isotope effect on the methanation reaction rate are reported in this study over a polycrystalline nickel foil at low total reactant pressure (5 Torr) and high H_2/CO ratio (15/1). Our measurement indicates that a kinetic isotope effect is observable for these reaction conditions.

In interpreting these data we will consider the possibility that the temperature and partial-pressure dependence of the surface concentrations of the adsorbed reactants strongly influences the observed kinetics. Atmospheric-pressure studies of hydrogen and carbon monoxide coadsorption (*17*) at room temperature and above have shown that the nickel surface is capable of adsorbing nearly monolayer concentrations of hydrogen and carbon monoxide simultaneously. These studies indicate, however, that partial precoverage of the nickel surface by CO increases the heat of adsorption of hydrogen on the nickel surface resulting in a slightly more tightly bound (3–5 kcal/mole) chemisorbed state. In contrast, hydrogen adsorption on a surface presaturated with CO at 273 K is substantially weakened. Although H_2 adsorbs, adsorption is endothermic and the hydrogen can be easily pumped away at room temperature (*17*). There observations define at least two states of adsorbed hydrogen, a weakly bound state adsorbing on regions of the nickel surface saturated by CO and a second tightly bound state adsorbing to the nickel atoms through a steady-state concentration of vacancies in the nearly saturated CO overlayer. The surface concentration of both states must be considered in understanding the observed kinetic behavior. The surface concentration of the tightly bound state of hydrogen absorbing through the steady-state concentration of vacancies or defects in the CO overlayer will be shown to be a strong function of both the partial pressure of the reactants and the temperature. The observed kinetic behavior of the methanation reaction will be shown to parallel in all essential respects the expected temperature and partial-pressure dependence of the hydrogen surface concentration in this tightly bound state. On the basis of these observations we propose that the active site at which the initiation of the synthesis reaction occurs is the hydrogen atom adsorbed through vacancies in a nearly saturated CO overlayer on the nickel surface.

EXPERIMENTAL PROCEDURES

Kinetic studies over polycrystalline nickel foils were carried out in the apparatus shown in Fig. 1. The apparatus consists of two ultrahigh vacuum (UHV) chambers connected by a differentially pumped gate valve and a UHV compatible transfer device. The transfer device has been previously described (*9*). The main UHV chamber is maintained at a base pressure below 1×10^{-10} Torr by liquid N_2-trapped Hg diffusion pumps. The UHV chamber is equipped with a PHI Auger spectrometer and an argon ion sputtering gun for sample cleaning and surface characterization as well as a UTI 100 quadrupole mass spectrometer and

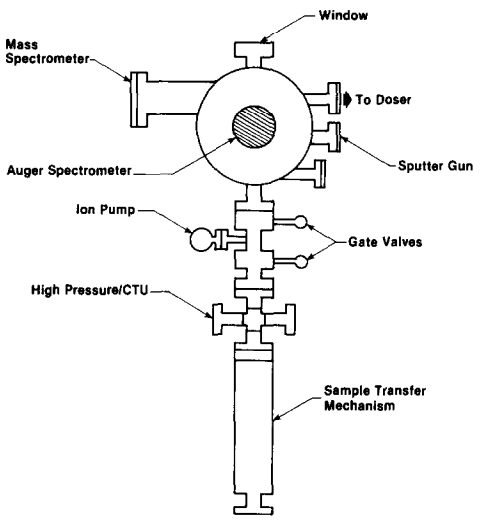

FIG. 1. Schematic view of the combined high-pressure reaction system and UHV electron spectrometer.

gas dosing needle. The 5.75-cm^2 Marz-grade polycrystalline nickel ribbon used in these studies (0.127 mm in thickness and 3.175 mm wide) was obtained from Materials Research Company. The ribbon was spot-welded to 3.175-mm-diameter Marz-grade nickel rods mechanically clamped to copper feedthroughs at the end of the transfer device. The sample is resistively heated. Sample temperature is monitored by a 3-mil tungsten/tungsten–26% rhenium thermocouple spot-welded to the center of the nickel foil. The high-pressure reactor portion of the apparatus consists of a short UHV nipple with four mini side ports for gas inlet and connections to the gas chromatograph and mass spectrometer. A schematic diagram of the reactor portion of the apparatus is shown in Fig. 2. The reactor walls are water cooled. With the sample fully retracted into the reactor and the gate valve closed, the rear of the sample mount seals the reactor from the metal bellows portion of the transfer device. This minimizes the reactor volume (75 cm^3) and allows reactor pressures up to 3 atm to be used. Gases for reaction and sample cleaning are inlet into the reactor from a separately pumped gas manifold. Spectroscopically pure Ar, H_2, and O_2 in 1-liter glass flasks are used for sample cleaning. The H_2/CO and D_2/CO mixtures used in these kinetic studies were obtained, premixed and spectroscopically analyzed, from Scientific Gas Products. The mixtures were stored in 500-cm^3 stainless-steel cylinders from which the gas could be metered directly into the UHV gas manifold.

In transferring the reaction gas mixtures from the gas manifold to the reactor the gases were passed over a copper sieve held at 200°C in order to decompose any carbonyl contaminants which might be present in the gas mixture. Auger analysis of the nickel ribbon catalyst after reaction in mixtures pretreated in this way showed no evidence of metal contamination from carbonyl decomposition. The reactor gas pressure was monitored by capacitance manometers attached to the inlet gas line as shown in Fig. 2. The gas composition in the reactor was continuously sampled through a quartz capillary into a separately pumped quadrupole mass spectrometer. The sampling system was calibrated in separate experiments to account for mass transport effects in the capillary. In these calibration experiments the response of the mass spectrometer was measured as a function of the partial pressure of D_2, H_2, CO, CH_4, and

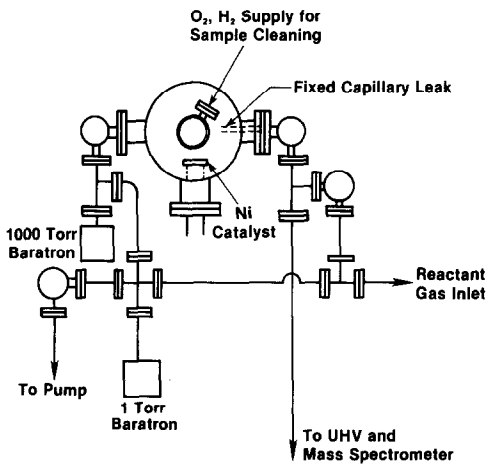

FIG. 2. Schematic diagram of the high-pressure reactor and associated gas mixing and sampling apparatus.

CD_4 in gas mixtures in the reactor. All data reported have been corrected for the mass transport properties of the sampling system.

The polycrystalline nickel foils used in these measurements were first outgassed under vacuum at 1000°C (several hours) until the base pressure of the UHV chamber returned to 10^{-10} Torr. The sample was then retracted into the reactor section where the sample was heated in flowing oxygen at a pressure of 1×10^{-5} Torr for 20 min followed by hydrogen reduction at a pressure of 5 Torr for 15–20 min. Following each cycle, the sample was transferred into the UHV chamber and the surface composition was monitored by Auger spectroscopy. These oxidation/reduction cycles were continued until the surface remained free of sulfur and carbon contamination when the sample was heated under vacuum to the maximum reaction temperature used in these measurements for periods of up to 30 min. A typical Auger spectrum of the clean nickel foil is shown in Fig. 3. A small residual oxygen peak in this figure amounting to <1% of a monolayer of oxygen on the nickel could not be removed. The chemical cleaning described above was preferred to sputter cleaning in the UHV system since the oxidation/reduction cycles clean both sides of the sample. After cleaning, the nickel foil is retracted into the reactor and the reaction gas mixture admitted. The sample temperature is stepped to the reaction temperature desired and the response of the quadrupole mass spectrometer for the mass 15 peak of CH_4 is monitored continuously in time. A typical kinetic run shown in Fig. 4 consists of heating the sample stepwise up and down in 20°C intervals from 160 to 400°C.

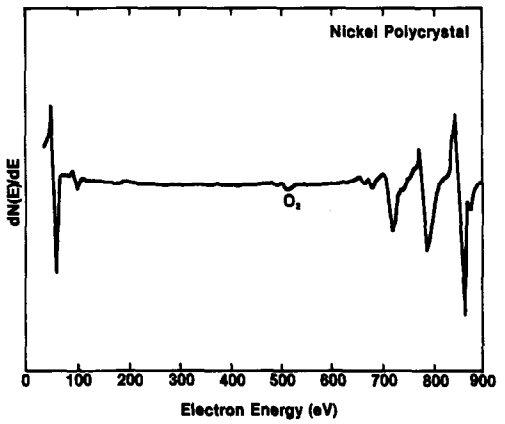

FIG. 3. An Auger spectrum of the clean nickel foil prior to reaction in CO/H_2 mixtures and following sequential oxidation and reduction to remove carbon and sulfur contamination.

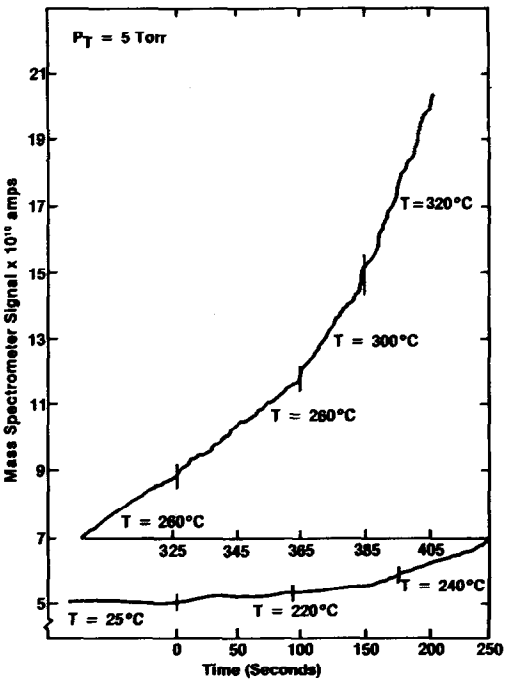

FIG. 4. The variation of the intensity of the mass 15 peak height with time on step heating the nickel foil in 20°C intervals at a total pressure of 5 Torr and at a H_2/CO ratio of 3/1. The Arrhenius plots of reaction rate versus $1/T$ are obtained by least-squares fitting these data to straight line segments.

RESULTS

Kinetic Studies on Polycrystalline Nickel Foils

Using the geometric surface area of the ribbon, and the calibration data relating mass spectrometer signal to CH_4 pressure in the reactor, the data can be expressed in the usual Arrhenius plot shown in Fig. 5.

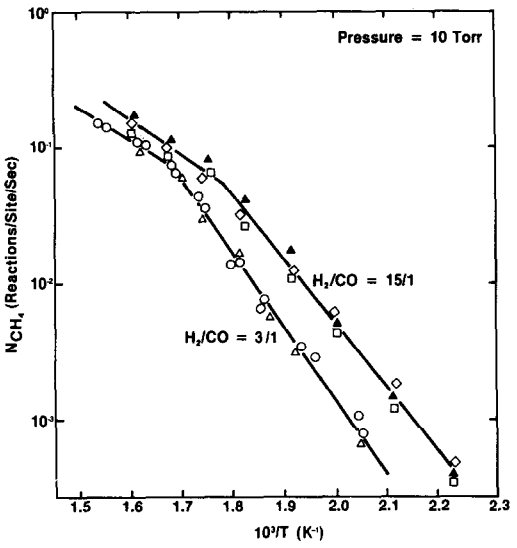

FIG. 5. The variation of the methanation rate with temperature for H_2/CO ratios of 3/1 and 15/1 at a fixed total reactant pressure of 10 Torr. The figures show that at fixed total pressure, the deviation from linear Arrhenius behavior with increasing temperature occurs at higher temperatures as the H_2/CO ratio increases. In addition, the data illustrate that the activation energy for methanation, at fixed total reactant pressure. decreases as the H_2/CO ratio increases.

The data of Fig. 5 are typical of the kinetic behavior of the methanation reaction over this polycrystalline nickel foil. For the experimental conditions shown in the figure, two kinetic regimes characterized by different apparent activation energies are evident. Provided the reaction temperature was maintained below 600 K the transition between the two kinetic regimes was entirely reversible. At higher temperatures (dependent on the H_2/CO ratio and total pressure) the reaction rate peaks. The specific reaction rate declines on further increasing the sample temperature and the foil reactivity is permanently poisoned. The studies described here are carried out exclusively in the regime of temperature, pressure, and H_2/CO ratio where the kinetic data are reversible. Several features of the kinetic behavior illustrated in Fig. 5 should be noted. The activation energy for the methanation reaction changes as a function of the reaction temperature. For a H_2/CO ratio of 15/1 at 5 Torr total reactant pressure, the activation energy decreases from 21.5 ± 0.5 kcal/mole at temperatures below 540 K to 14.2 ± 0.5 kcal/mole at higher temperatures. This behavior is consistent with previously reported data on polycrystalline nickel foils and nickel single crystals (*10–14*) and is in agreement with data obtained on high-surface-area nickel powders (*11*). Comparison of the data in Fig. 5 for H_2/CO ratios of 3/1 and 15/1 shows that at a fixed total pressure of the reactants the temperature at which the transition occurs (defined by the intersection of the linear Arrhenius plots in the high and low temperature regimes) shifts to a lower value as the H_2/CO ratio increases. This shift to lower temperature as the H_2/CO ratio increases is again consistent with previously reported data on nickel powders (*11*).

The partial-pressure dependence of the methanation reaction rate on these poly-

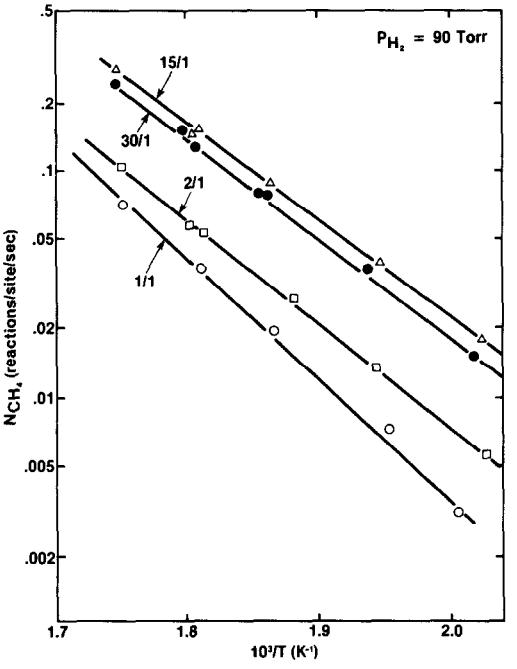

FIG. 6. Arrhenius plots of the methanation activity of a polycrystalline nickel foil as a function of the H_2/CO ratio at a fixed hydrogen partial pressure of 90 Torr. Isothermal cuts through these data yield the CO partial-pressure dependence of the reaction.

crystalline nickel foils was obtained in the usual way by fixing the partial pressure of either CO or H_2 and varying the total reactant pressure and H_2/CO ratio. The results in Figs. 6 and 7 illustrate the CO and H_2 partial-pressure dependence of the reaction rate for a fixed hydrogen pressure of 90 Torr and a fixed carbon monoxide partial pressure of 6 Torr, respectively. The data are obtained for temperatures below the transition. Even for temperatures well below the transition, the apparent activation energy of the reaction is found to be a function of the H_2/CO ratio. Table 1 summarizes these results. In each case, the total conversion based on the CH_4 concentration in the reaction gas was maintained below 1%. The activation energy for the reaction at comparable total pressure decreases from 24.5 ± 0.5 to 19.6 ± 0.5 kcal/mole as the H_2/CO ratio increases from 1/1 to 30/1. In contrast, the apparent activation energy is nearly independent of the total reactant pressure at constant H_2/CO ratio within experimental error.

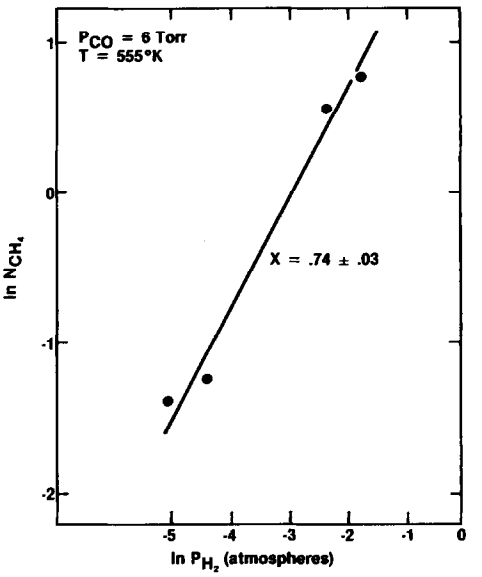

FIG. 8. Hydrogen pressure dependence. Plot of the log of the methanation activity versus the log of the hydrogen partial pressure obtained from an isothermal cut through the data of Fig. 6 at 555 K. The slope of the line least-squares fit to this data yields the order of the reaction on hydrogen.

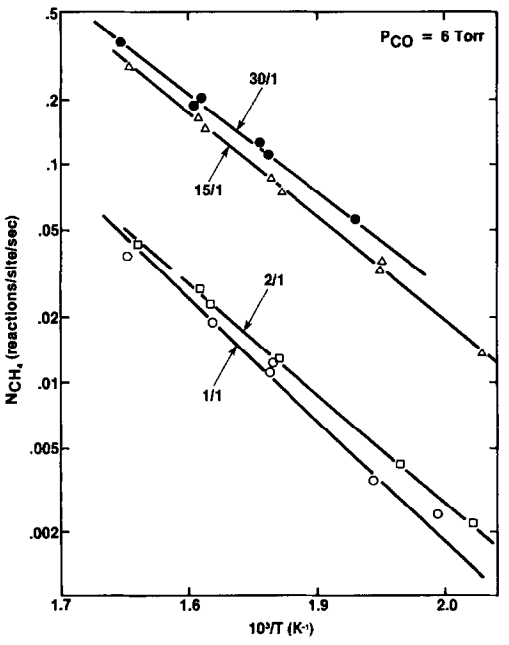

FIG. 7. Arrhenius plots of the methanation activity of a polycrystalline nickel foil as a function of the H_2/CO ratio at a fixed CO partial pressure of 6 Torr. Isothermal cuts through these data yield the hydrogen partial-pressure dependence of the reaction.

The usual methods used to obtain the partial-pressure dependence of the reaction as expressed in the form

$$N_{CH_4} = A\, P_{H_2}{}^{x} P_{CO}{}^{y} \exp -\Delta H_{CH_4}/RT \quad (1)$$

assume that the activation energy H_{CH_4} and the orders of the reaction x and y are inde-

TABLE 1

Summary of Apparent Activation Energy for Methanation over Ni Foil

H_2/CO ratio	P_T (Torr)	E_m (kcal/mole)
1/1	180	24.3 ± 0.5
1/1	10	24.2 ± 0.5
2/1	15	22.9 ± 0.5
15/1	80	21.7 ± 0.5
2/1	135	21 ± 0.5
30/1	93	20.6 ± 0.5
15/1	96	19.9 ± 0.5
30/1	155	19.6 ± 0.5

pendent of the H_2 and CO partial pressures and temperature. The data in Table 1 clearly show that this is not the case. It is well recognized that Eq. (1) is an empirical correlation of the experimental data where the parameters x and y are valid only for the particular conditions for which they are measured. In any heterogeneously catalyzed reaction it is the surface concentrations and not the partial pressures of the reactants which should appear in Eq. (1). When x and y are taken as constants it implies that the surface concentrations of the surface species are proportional to a simple fixed power of the gas-phase partial pressures. This is clearly not correct and we must expect that x and y will be functions of T, P_{CO}, and P_{H_2}. Taking a vertical cut through the data of Figs. 6 and 7 at a temperature of 555 K and plotting the resulting in N_{CH_4} versus the corresponding ln P_{H_2} and ln P_{CO}, respectively, we obtain the plots in Figs. 8 and 9. The slopes of these plots yield values of the orders on hydrogen partial pressure $x = 0.74 \pm 0.03$ and carbon monoxide partial pressure $y = -0.43 \pm 0.03$ in good agreement with values previously reported on both supported and unsupported nickel catalysts as shown in Table 2.

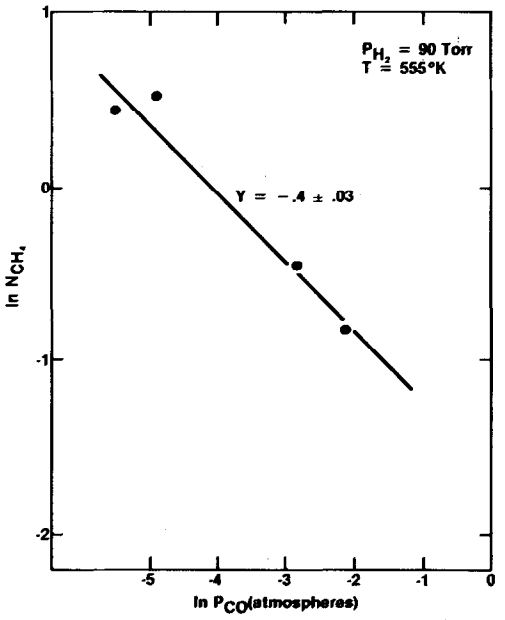

FIG. 9. CO pressure dependence. Plot of the log of the methanation activity versus the log of the carbon monoxide partial pressure obtained from an isothermal cut through the data of Fig. 7 at 555 K. The slope of the line least-squares fit to this data yields the order of the reaction on carbon monoxide pressure.

TABLE 2

Summary of Pressure Dependency

Catalyst	Pressure range (Torr)	x	y
5% Ni/Al_2O_3	600–760	0.77 ± 0.04	−0.31 ± 0.05
Ni powder	600–760	1.0 ± 0.04	−0.4 ± 0.05
Ni foil	1–400	0.74 ± 0.03	−0.4 ± 0.03

If x and y are indeed constants at a given temperature, then the sum of the orders of the reaction $(x + y) = 0.34 \pm 0.6$ obtained from Eq. (1) by the method described above must agree with the sum of the orders of the reaction $(x + y)$ obtained from Eq. (1) by fixing the H_2/CO ratio and varying the total reactant pressure over the same pressure range. In particular, from Eq. (1) if $P_{H_2}/P_{CO} = r$(constant) then

$$N_{CH_4} = Ar^x P_{CO}^{(x+y)} \exp -\Delta H_{CH_4}/RT$$

and

$$\ln N_{CH_4} = (-\Delta H_{CH_4}/RT + \ln Ar^x) + (x + y) \ln (P_{CO}).$$

Since ΔH_{CH_4} and r are constant for a fixed H_2/CO ratio, and A and x are also assumed to be constant, a plot of ln N_{CH_4} vs ln (P_{CO}) would yield a straight line whose slope is equal to the sum of the orders of the reaction $(x + y)$. Figure 10 shows a plot of the ln N_{CH_4} versus ln P_{CO} for a H_2/CO ratio of 15/1 at 555 K. The slope of this curve varies from 0.12 to 0.70 as the reactant pressure increases from 10 to 200 Torr. Since the slope is not constant, the sum of the reaction orders $(x + y)$ cannot be obtained by varying the total pressure at fixed H_2/CO

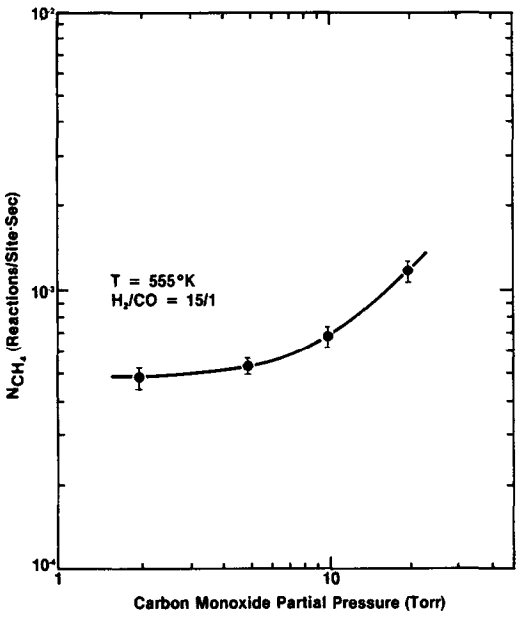

FIG. 10. Variation of the methanation rate with CO partial pressure at a fixed H_2/CO ratio of 15/1 and fixed temperature of 555 K. If the orders of the reaction x and y were constant over the range of reaction conditions used in these experiments, the data should be a straight line with a slope equal to the sum of the orders $(x + y)$.

ratio as in Fig. 10 except for the case where $r = 1$.[2]

For the purpose of modeling the mechanism of the methanation reaction, the values of x and y obtained in this way have little or no significance since the isotherm for the competitive adsorption of H_2 and Co is not known. The variation of the orders of the reaction x and y with temperature, CO partial pressure, and H_2 partial pressure over a wide range of reaction conditions would, however, provide an important criterion against which to compare the validity of any proposed mechanism.

Kinetic Isotope Effect

If hydrogen participates in the rate-limiting step of the methanation reaction, a kinetic isotope effect may be observed when the hydrogen in the reaction mixture is replaced by deuterium, all other reaction parameters remaining constant. Failure to observe a kinetic isotope effect, as pointed out by Ozaki and later by Wilson does not, however, conclusively show that hydrogen does not participate in the rate-limiting step. They point out that cancellation of the kinetic and thermodynamic isotope effects may result in a net effect which is too small to be observable over the range of conditions used in typical kinetic studies. Wilson suggests that this cancellation is responsible for the failure of Dalla Betta and Shelef to observe a kinetic isotope effect in the methanation reaction. The proposed cancellation is of course critically dependent on the kinetics of the competitive adsorption of H_2 and CO on the catalyst surface. If the kinetic limitations on the competitive adsorption are a function of the reaction conditions as we expect, a measurable kinetic isotope effect may be observable if the reaction conditions are varied over a wide enough range of pressure, H_2/CO ratio, and temperature. For measurements of the kinetic isotope effect in these studies the mass spectrometer sampling capillary in our reactor was independently calibrated with both H_2/CO/CH_4 and D_2/CO/CD_4 mixtures. For calibration purposes, H_2/CO/CH_4 and D_2/CO/CH_4 gas mixtures were prepared in the reactor spanning the range of the CH_4 and CD_4 pressures in the reaction mixture during the kinetic studies. CH_4 and CD_4 gas pressures in the reactor were measured by a 1-Torr capacitance manometer

[2] It has been suggested that the surface is saturated in both carbon monoxide and hydrogen. The data presented above are inconsistent with this postulate. If the surface were saturated, the orders of the reaction in both hydrogen and carbon monoxide would indeed be independent of the reaction conditions and the orders obtained by the two methods described above would agree. This is clearly not the case for the polycrystalline nickel foil used in these studies. The confusion may arise from the fact that the previously reported zero-order reaction kinetics in hydrogen partial pressure (*14*) were calculated from the measured order in CO partial pressure and the sum of the orders obtained by varying the total pressure at fixed H_2/CO ratio. As we have pointed out above, this approach is valid only if the sums of the orders obtained by the two methods are in agreement over the range of the data collected.

(MKS-314BH) and the H_2/CO and D_2/CO mixture gas pressures by a 10-Torr capacitance manometer (MKS-221AHS) mounted directly on the reactor. For each mixture prepared in this way, the response of the sampling system was calibrated for fixed mass spectrometer settings. In each case, the pressure at the mass spectrometer was maintained below 1×10^{-8} Torr and minor variations in mass spectrometer sensitivity from day to day were compensated by normalizing the spectra to the CO peak height. Figure 11 shows data for the kinetic isotope effect for H_2/CO and D_2/CO ratios of 15/1 and a total reactant pressure of 5 Torr. Data points shown in the figure are for both increasing and decreasing catalyst temperature and include data points from independent experiments with cleaning of the nickel foil catalyst between each kinetic run. A kinetic isotope effect is indeed evident from the data. The enhancement of the specific activity for normal methane production over that for the production of deuterated methane is $N_{CH_4}/N_{CD_4} = 1.86 \pm 0.2$ while the activation energy, $\Delta H_{CH_4} = 23 \pm 2$ kcal/mole, is unchanged within experimental error.

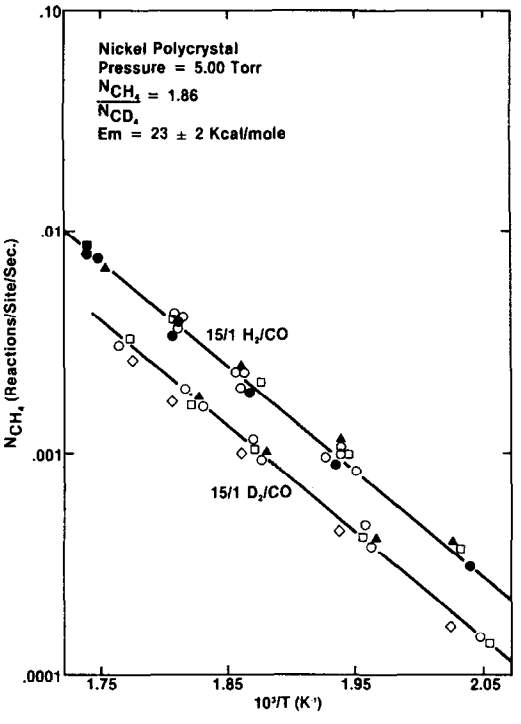

FIG. 11. Arrhenius plots of the methanation rate versus $1/T$ for a fixed reactant pressure of 5 Torr. The upper curve is for a H_2/CO ratio of 15/1. The lower curve is for a D_2/CO ratio of 15/1. The data show the existence of a kinetic isotope effect in the methanation activity of this polycrystalline nickel foil for these reaction conditions.

Summary of Kinetic Behavior

These kinetics studies show that two reversible regions of kinetic behavior exist for the methanation reaction. The transition between these two kinetic regimes is characterized at fixed reactant pressure and H_2/CO ratio by a change in both the apparent activation energy of the reaction and the partial-pressure dependence of the reaction rate (*11*). The transition temperature, defined by the intersection of the two linear Arrhenius regions, shifts to lower temperature as the H_2/CO ratio increases. At temperatures below the transition the observed activation energy of the methanation reaction is dependent on the H_2/CO ratio but is independent of total reactant pressure over the range of pressures studied. Comparison of the reaction orders obtained by varying the total reactant pressure shows that the reaction orders are not constant over the range of experimental conditions used. Finally, at low pressure and high H_2/CO ratio, a kinetic isotope effect is observed in the methanation reaction rate.

DISCUSSION

It is clear from the kinetic data that over the range of experimental conditions used in these studies neither the orders of the reaction on H_2 and CO partial pressures nor the activation energy of the reaction are constant. This might, of course, be interpreted to mean that a single rate-limiting step for the methanation reaction does not exist and we are in fact observing the superposition of a number of competing processes. This possibility cannot be discounted. If, however, we assume that a

unique rate-limiting step does exist for this reaction, which gives rise to the observed kinetic behavior, then it is relevant to ask how much of the observed kinetics is associated with the changes of the surface concentrations of the reactants.

We will show below that much of the observed kinetic behavior of the methanation reaction can be attributed to the temperature and partial-pressure dependence of the hydrogen and carbon monoxide surface concentrations. Any complete description of the reactant surface concentration must, of course, take into account not only the hydrogen and carbon monoxide surface concentration but also the carbon surface concentration arising from the dissociation or disproportionation of the CO in the presence of hydrogen (*20–23*). Such a detailed analysis will have to await data on the disproportionation kinetics of CO on the nickel surface beyond what is currently available. For the moment, we will concern ourselves with the competition between hydrogen and carbon monoxide on the metal surface which is not already occupied by carbon. Neglecting the carbon surface concentration as a first approximation will be valid provided that the variation of at least one of the reactants on the surface is large in comparison to the variation of the surface carbon concentration as the reaction conditions are varied. This approach is motivated by the fact that the surface under reaction conditions is nearly saturated with either carbon monoxide or a mixture of carbon monoxide and carbon and the reported variation of the carbon surface concentration with reaction temperature is small in the linear Arrhenius region below the transition. Since methanation is a hydrogenation reaction, it is interesting to consider whether or not the methanation reaction rate may be limited by the hydrogen concentration available on the surface. The variation of the surface concentration of hydrogen in competition with carbon monoxide on the metal surface not occupied by carbon should then correlate directly with the observed methanation reaction kinetics provided that the variation in hydrogen surface concentration on the exposed metal is large in comparison to the change in carbon concentration (i.e., availability of metal surface) over the range of reaction conditions studied.

In constructing a model for the hydrogenation of CO to methane we will begin by writing steady-state relations for the surface concentrations of H_2 and CO. Using these relations, we will examine the dependence of the H_2 and CO surface concentrations on pressure and sample temperature.

For the moment, we need to write expressions for the surface concentration of CO molecules and H atoms as a function of: the CO pressure, the H_2 pressure, and the surface and gas temperature. We will assume that the surface concentrations of H and CO are in the steady state with the H_2 and CO in the gas phase. We further assume that a CO molecule will displace a pair of H atoms adsorbed on the surface, but a H_2 molecule will not displace an adsorbed CO molecule. The latter assumption is in accord with the experimentally observed behavior at high pressure and elevated temperatures (*15*).

The CO surface concentration can then be calculated as if the surface were free of adsorbed H_2. In the steady state,

$$\phi_{CO} S_0^{CO}(1 - N^{CO}/N) = N^{CO}\nu_0^{CO} \exp -(H_D^{CO}/KT_s), \quad (2)$$

where the right side of Eq. (2) is the rate of desorption of CO per square centimeter and the left side is the rate of adsorption of CO per square centimeter. S_0^{CO} is the zero-coverage sticking coefficient for CO, $\phi_{CO} = P_{CO}/(2\pi m_{CO} KT_g)^{1/2}$ is the ideal gas impingement rate for a CO pressure P_{CO}, ν_0^{CO} is the frequency with which the CO molecules try to leave the surface, ΔH_D^{CO} is the activation energy for desorption of CO, and N^{CO} and N are, respectively, the surface concentration of CO in molecules per square centimeter and the total number of adsorption sites per square centimeter. Rearranging

Eq. (2) gives

$$N^{CO} = \frac{K^{CO}}{1 + K^{CO}/N}, \quad (3)$$

where

$$K^{CO} = \frac{\phi_{CO} S_0^{CO}}{\nu_0^{CO}} \exp(\Delta H_D^{CO}/KT_s).$$

Equating the rate of adsorption of H_2 to the rate of desorption in the steady state we obtain

$$\left(\frac{N^H}{N}\right)^2 \nu^H \exp -(\Delta H_D^H/KT_s) + \phi_{CO} S_0^{CO} \left(\frac{N^H}{N}\right)^2 = \phi_H S_0^H \left(1 - \frac{N^{CO}}{N} - \frac{N^H}{N}\right)^2. \quad (4)$$

The first term on the left side is the rate of desorption of H_2 due to recombination of H atoms, ν^H is the collision frequency of H atoms, and ΔH_D^H is the activation energy for thermal desorption of H_2. The second term on the left side is the rate of displacement of hydrogen from the surface by the adsorbing CO molecules and the right-hand expression is the rate of adsorption of hydrogen molecules from the gas phase on that portion of the surface which is not already occupied by an adsorbed CO molecule. From Eq. (4) we obtain

$$N^H = \frac{GN'}{G'N + G}, \quad (5)$$

where

$$N' = N - N^{CO},$$

$$G = \frac{\phi^H S_0^H}{\nu^H} \exp +(\Delta H_D^H/KT),$$

$$G' = \frac{\phi_{CO} S_0^{CO}}{\nu^H} \exp + (\Delta H_D^H/KT).$$

ϕ_H, S_0^H, and N^H are as before the ideal gas impingement rate, zero-coverage sticking coefficient, and surface concentration of hydrogen atoms per square centimeter. We will approximate the collision frequency $\nu^H = 2^{1/2}\sigma_0 (\pi KT_s/2m_H)^{1/2}$, where σ_0 is the hard-sphere collision diameter of the migrating adatoms.

The dependence of the H and CO surface concentrations on the H_2 and CO partial pressures and sample temperature is determined by applying literature values (*17–19*) of the initial sticking coefficients and desorption energies for H_2 and CO on nickel.

Figure 12 shows the dependence of the CO surface concentration on the CO and H_2 partial pressures at a surface temperature of 500 K. The H_2/CO ratios and total reactant pressures represented in Fig. 12 ($2.0 \leq H_2/CO \leq 20.0$; 150 Torr $\leq P_T \leq$ 1000 Torr) span the ranges normally used in kinetic studies of methanation over nickel. The calculations show that at 600 K the surface remains nearly saturated with CO ($0.97 \leq \theta \leq 0.99935$) as the H_2/CO ratio varies from 50/1 to 0.5/1 at a total reactant pressure of 760 Torr. As the catalyst temperature is raised, the CO surface concentration at fixed H_2/CO ratio, as shown in Fig. 12, decreases due to increase thermal desorption of the molecularly bound CO. The decrease in the CO surface concentration with increasing temperature is small over the range of typical reaction conditions. For a H_2/CO ratio of 0.5/1 at a total pressure of 760 Torr the

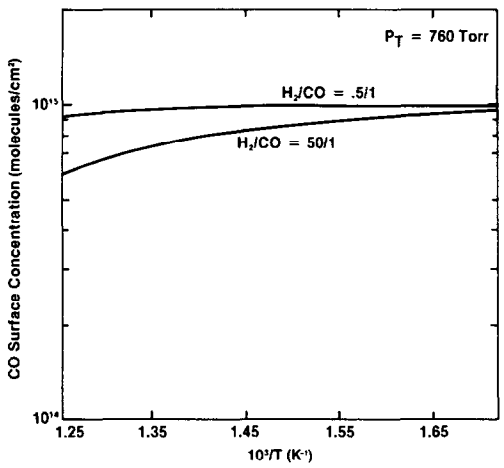

FIG. 12. The calculated variation of the carbon monoxide surface concentration with temperature and H_2/CO ratio for a fixed total reactant pressure of 760 Torr. The data show that for all realistic methanation reaction conditions, the surface is close to saturation with carbon monoxide. The concentration of vacant sites is a strong function of temperature and H_2/CO ratio.

carbon monoxide surface coverage varies from $\theta = 0.99996$ to $\theta = 0.980$ as the catalyst temperature varies from 500 to 700 K. This apparently insignificant change in the carbon monoxide surface concentration represents, however, a three-order-of-magnitude increase in the metal surface area available for hydrogen chemisorption.

Figure 13 illustrates the dependence of the H-adatom surface concentration on the hydrogen and CO partial pressures at 500 K. The data are, again, for H_2/CO ratios and reactant pressures typically used in kinetic studies of methanation. The H-adatom surface concentration in Fig. 13B shows an approximately inverse first-order dependence on the carbon monoxide partial pressure. This behavior reflects the strong inhibition of hydrogen chemisorption on nickel by the adsorbed carbon monoxide. By comparison, the dependence of the H-adatom surface concentration on the hydrogen partial pressure, shown in Fig. 13A, is quite weak. Over the range of conditions shown, the dependence of the H-adatom surface concentration on the hydrogen partial pressure only varies from $P_H^{0.15}$ to $P_H^{0.20}$. This weak dependence on the hydrogen partial pressure arises from the fact that although the H-adatom surface concentration is small, the surface available for hydrogen chemisorption is nearly saturated with hydrogen. The isotherm for dissociative hydrogen chemisorption on nickel is half-order in hydrogen partial pressure only in the limit of low coverage on the available surface and decreases to zero order in hydrogen partial pressure as the available surface area approaches saturation. For realistic reaction conditions, the H-adatom surface concentration is always far from the dilute limit on the available surface area.

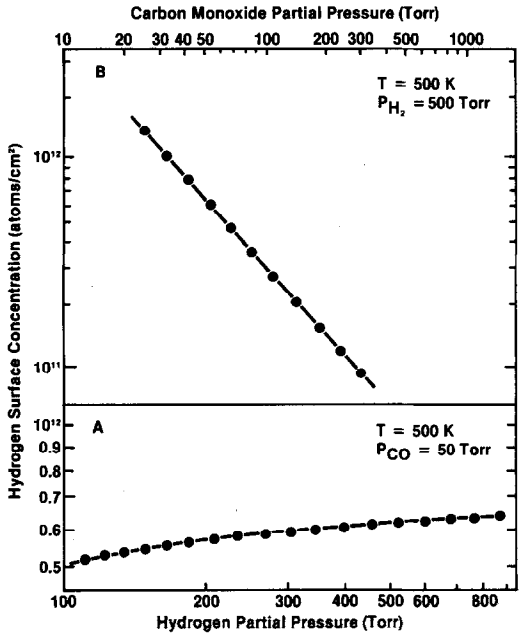

FIG. 13. (A) The calculated variation of hydrogen surface concentration with hydrogen partial pressure for a fixed CO pressure of 50 Torr and a constant temperature of 500 K. The plot shows that the steady-state surface concentration of hydrogen in this strongly bound state is small ($5 \times 10^{-4} \leq \sigma_H \leq 7 \times 10^{-4}$) for realistic methanation reaction conditions and that the hydrogen partial-pressure dependence of the surface concentration is weak. (B) The calculated variation of the hydrogen surface concentration with CO pressure for a fixed hydrogen pressure of 500 Torr and a fixed temperature of 500 K. The plot illustrates the nearly inverse first-order dependence of the hydrogen surface concentration in this tightly bound state on the CO partial pressure.

The temperature dependence of the H-adatom surface concentration in the limits of high and low H_2/CO ratios and at a total reactant pressure of 760 Torr is illustrated in Fig. 14. The calculated temperature dependence of the H-adatom surface concentration parallels the observed kinetics of the methanation reaction. The hydrogen surface concentration is strongly dependent on temperature at both high and low H_2/CO ratios. Displayed as an Arrhenius plot, the H-adatom concentration shows two distinct limiting behaviors. In the low temperature regime, the temperature dependence of the H-adatom surface concentration shows an approximately linear Arrhenius behavior with an effective activation energy which decreases from 20.18 to 13.27 kcal/mole as the H_2/CO ratio increases from 0.5/1 to 50/1. In the low temperature regime the temperature dependence of the surface hydrogen concentration is dominated by the

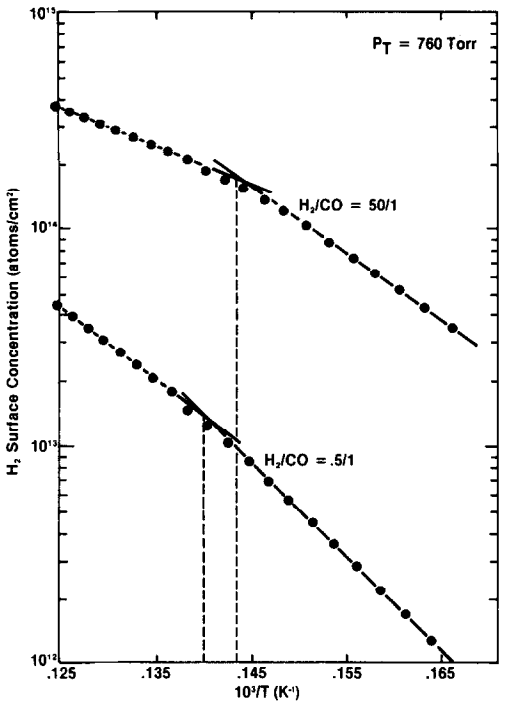

FIG. 14. The calculated dependence of the hydrogen surface concentration on temperature and H_2/CO ratio at a fixed total reactant pressure of 760 Torr. This plot illustrates that the variation of the hydrogen surface concentration with temperature and H_2/CO ratio in this state parallels the observed kinetics of the methanation reaction on the nickel surface.

change in the surface area available for hydrogen chemisorption due to thermal desorption of CO. In addition a contribution of a certain amount of the adsorption/desorption character of the hydrogen is also mixed into the total temperature dependence and the magnitude of this contribution increases as the H_2/CO ratio increases. The increased contribution of the hydrogen desorption character with increased H_2/CO ratio is responsible for the shift in the apparent activation energy to lower values as the H_2/CO ratio increases.

In the limit of high temperatures the CO surface concentration decreases and the temperature dependence of the H-adatom surface concentration becomes dominated by the hydrogen adsorption/desorption character. The increased contribution of the hydrogen adsorption/desorption character with increasing temperature gives rise to the decreases in apparent activation energy with increasing temperature. The transition between these two limiting behaviors, as expected, shifts to lower temperatures as the H_2/CO ratio increases.

The behavior of the hydrogen surface concentration described above is insensitive to the values of the parameters for hydrogen adsorption used in the calculations for the competitive adsorption of hydrogen and CO on the nickel surface. Quantitatively, the temperature of the transition between the regimes, the functional form of the dependence of the transition temperature with H_2/CO ratio and total pressure, the values of the activation energies above and below the transition, and the details of the partial-pressure dependences are strongly dependent on the magnitude and coverage dependence of the CO desorption energy close to saturation. It is this parameter which controls the amount of surface area available for H_2 chemisorption. Since detailed data are not available for the coverage dependence of the CO heat of desorption at $\theta_{CO} > 0.60$, quantitative comparison of the calculated temperature dependence of the H-adatom concentration with the measured kinetics of the methanation reaction is not meaningful.

Qualitatively, the temperature dependence of the calculated hydrogen-adatom surface concentration described above is the same as the experimentally observed temperature dependence of the methanation reaction rate. Combined with the observation of a kinetic isotope effect for the methanation reaction rate, our results strongly suggest that the methanation reaction on nickel is a hydrogen surface concentration-limited reaction, the majority of the observed kinetics being controlled by the temperature and partial-pressure dependence of the surface concentration of hydrogen in the primary chemisorbed layer.

A variety of kinetic models have been proposed for the hydrogenation of CO to methane on the nickel surface. In every

case, except the unpromoted dissociation of CO, these mechanisms invoke a rate-determining step involving either the hydrogenation of a surface species or the hydrogen promotion of the dissociation of carbon monoxide. Our suggestion, that the controlling factor in the observed kinetics of methanation is the temperature and partial-pressure dependence of the H-adatom surface concentration in the primary chemisorbed layer, is compatible with any mechanism which invokes either a surface hydrogenation or hydrogen-promoted dissociation as the rate-determining step in the reaction. The unpromoted dissociation or disproportionation of CO as the rate-limiting step on nickel is not consistent with our observations. Measurements of the kinetics of the disproportionation of CO over evaporated nickel film and supported nickel catalysts have shown that for typical reaction conditions, the unpromoted rate of CO disproportionation is too slow to account for the rate of formation of methane (*16*). This conclusion is supported by our observation of a kinetic isotope effect at low pressure and high H_2/CO ratios observed over these polycrystalline nickel foils. This observation clearly indicates that hydrogen is influencing the rate-determining step of the reaction.

The state of hydrogen which we have been discussing, that is, hydrogen chemisorbing to the initial surface through vacancies or defects in the chemisorbed CO overlayer, cannot, by itself, fully account for the observed reaction kinetics. In particular, the surface concentration of this primary chemisorbed state does not exceed a few percent of a monolayer for realistic reaction conditions and the partial-pressure dependence of the H-adatom surface concentration in this state ($P_{H_2}^{0.15} - P_{H_2}^{0.20}$) is too small to account for the observed hydrogen partial-pressure dependence of the overall reaction. Numerous studies of coadsorption of H_2 and CO (*17, 18*) on supported and unsupported nickel catalysts show that at temperatures up to 50°C both a monolayer of CO and a monolayer of hydrogen coexist on the nickel surface in equilibrium with the gas. The vast majority of the hydrogen adsorbed in the presence of CO is, however, weakly bound and readily desorbs on evacuation at room temperature (*17*). These observations suggest that there are at least two states of hydrogen coadsorbed on the nickel surface, the primary chemisorbed state described above, adsorbing through vacancies or defects in the CO overlayer and acting as the initiation site for the reaction, and a second more weakly bound state of hydrogen in equilibrium with the gas and contributing to the hydrogenation of the reaction intermediates.

Our suggestion, that the hydrogen surface concentration is a strong function of reaction temperature at fixed total pressure and H_2/CO ratio, allows resolution of a number of key issues which have hampered identification of the reaction mechanism. In particular, in the case of the hydrogenation of an active surface carbon as the rate-determining step, the methanation of carbon by hydrogen is observed to occur at a faster rate and with lower activation energy (~17 kcal/mole) than the corresponding rate of methanation of CO on nickel catalysts (*16*). If the hydrogen surface concentration is rate limiting, the rate of hydrogenation of the active surface carbon at comparable carbon surface concentrations would be expected to be slower in the presence of CO, since the hydrogen surface concentration is reduced by competition with CO for the available metal sites. In addition, the observed activation energy for the reaction would be strongly influenced by the temperature dependence of the hydrogen surface concentration. As we have shown, the temperature dependence of the hydrogen surface concentrations below the transition is primarily controlled by the CO desorption energy (~26 ± 2 kcal/mole). Below the transition, an activation energy for the reaction between 13 and 20 kcal/mole is expected as a result of the temperature

dependence of the hydrogen surface concentration alone; further, our results suggest that the variation in activation energies reported for this reaction in the literature is not due to experimental error but is, at least in part, due to variations of the observed activation energy with reaction conditions. The lowering of the observed activation energy with increased H_2/CO ratio at fixed total pressure and temperature is again consistent with the ability of hydrogen to compete more effectively for surface sites.

REFERENCES

1. Vannice, M. A., *Catal. Rev. Sci. Eng.* **14,** 153 (1976).
2. Mills, G. A., and Steffgen, F. W., *Catal. Rev. Sci. Eng.* **8,** 159 (1973).
3. Vlasenko, J. M., and Yuzefovich, G. E., *Russ. Chem. Rev.* **38,** 728 (1969).
4. Dalla Betta, R. A., and Shelef, M., *J. Catal.* **49,** 383 (1977).
5. McKee, D. W., *J. Catal.* **8,** 240 (1967).
6. Sakharov, M. M., and Dokukina, E. S., *Kinet. Katal.* **2,** 710 (1961).
7. Ozaki, A., "Isotopic Studies of Heterogeneous Catalysis," p. 168. Academic Press, New York, 1977.
8. Wilson, T. P., *J. Catal.* **60,** 167 (1979).
9. Polizzotti, R. S., and Schwarz, J. A., *Rev. Sci Instrum.* **17**(2), 655 (1980).
10. Kelley, R. D., Reevesz, K., Madey, T. E., and Yates, J. T., Jr., *Appl. Surf. Sci.* **1,** 266 (1978).
11. Polizzotti, R. S. Schwarz, J. A., and Kugler, E. L., *in* "Proceedings of the Symposium on Advances in Fischer-Tropsch Chemistry." Amer. Chem. Soc., Annaheim, 1978.
12. Goodman, D. W., Kelley, R. D., Madey, T. E., and Yates, J. T., Jr., *in* "Proceedings of the Symposium on Advances in Fischer-Tropsch Chemistry." Amer. Chem. Soc., Annaheim, 1978.
13. Madey, T. E., Goodman, D. W., and Kelley, R. D., *J. Vac. Sci. Technol.* **16,** 433 (1979).
14. Goodman, D. W., Kelley, R. D., Madey, T. E., and Yates, J. T., Jr., *J. Catal.* **63,** 226 (1980).
15. Polizzotti, R. S., to be published.
16. Van Ho, S., and Harriott, P., *J. Catal.* **64,** 272 (1980).
17. Wedler, G., Papp, H., and Schroll, G., *J. Catal.* **38,** 153 (1975).
18. Wedler, G., Papp, H., and Schroll, G., *Surf. Sci.* **44,** 463 (1974).
19. Hogan, A. M., and King, D. A., *in* "Adsorption-Desorption Phenomena" (F. Ricca, Ed.), p. 329. London, 1972.
20. Araki, M., and Ponec, U., *J. Catal.* **44,** 439 (1976).
21. Madden, H. H., and Eril, G., *Surf. Sci.* **35,** 211 (1973).
22. Weytrcek, P. B., Wood, B. J., and Wise, H., *J. Catal.* **43,** 363 (1976).
23. Erley, W., and Wagner, H., *Surf. Sci.* **74,** 333 (1978).